May 10, 2000

Prof. Roni Avissar
Chief Editor, JGR-Atmospheres
Dept. of Environmental Sciences, Cook College - Rutgers University
New Brunswick, NJ 08903

Re: JGRd-2000R034 and 2000R035

Dear Roni,

Enclosed please find three copies of our revised two-part paper entitled *"A Catchment-Based Approach to Modeling Land Surface Processes in a GCM. Part 1: Model Structure. Part 2: Parameter Estimation and Model Demonstration."*. Our detailed response to the reviewers' comments is attached to this cover letter.

Thank you for your help with this one!

Sincerely,

Randal Koster
Hydrological Sciences Branch
Code 974, NASA/GSFC
Greenbelt, MD 20771
(301) 614-5781
(301) 614-5808 (FAX)
randal.koster@gsfc.nasa.gov

Responses to Reviewers

Reviewer A

1. Infiltration-excess overland flow *is* modeled in the LSM, as made clearer now in section 3.7 (Part 1). The fact that this type of overland flow contributed to the runoff we simulated in the Red Arkansas basin is now stated explicitly in section 4.1 (Part 2). Thus, we do not conclude that we are estimating the correct flow with the wrong processes.

2. We removed the contradictory words about runoff routing. The fact that a few SVATs performed as well as the catchment LSM in the Red Arkansas basin in PILPS2c, and what that implies about their relative merits, is now addressed in a paragraph in the conclusions section of Part 2.

3. A short paragraph addressing this is now included in the conclusions section of Part 2.

4. The reason for the apparent lack of sensitivity is simply that baseflow is not a significant component of the total runoff. This is stated in the second-to-last paragraph of section 4.3. In any case, we never mean to imply that runoff is not at all sensitive to the mean. The same paragraph now states this more clearly. We've also added a sentence about this in the conclusions.

5. Corrected.

6. Corrected.

7. Corrected – two references to eq. 16 were changed to eq. 11.

Reviewer B

General Comments. We disagree with the reviewer on this. Although the two parts obviously belong next to each other, they are distinct enough in both flavor and subject matter to maintain their separate identities. The first part argues the need for a topography-based model and then describes the overall structure of the particular model we designed. As a "philosophy" paper or as a model description paper, this part could stand alone. The second part is, in contrast, much more "technical" and addresses the many issues associated with actually implementing the model. It serves to demonstrate, through parameter analyses and offline simulations, that the catchment model is indeed viable.

While going back and forth between the two papers may, in one sense, be inconvenient, we feel that the reader will generally benefit from the separation of the overarching principles of the model (Part 1), which are complex in their own right, from the technical and operational problems faced when running the model efficiently (Part 2). Integrating the "theoretical" parameterizations in Part 1 with the "empirical" parameterizations in Part 2 (as suggested in the reviewer's comment #3) would, in our opinion, make the discussion more indigestible for the average reader, who may be mostly interested in one or the other.

1. To us, the text at the top of page 10 seems to fit in well where it is – it describes the main distinctions between our catchment model and the TOPLATS model as part of a paragraph that describes, in broader terms, how our model relates to other models in the literature. Our other responses to the earlier reviewers' comments also seem to be in the right places – in the places where the reviewers apparently noticed problems the first time. A careful reading of the manuscript suggests, to us, that our responses have been smoothly incorporated into the text.

2. Once again, we must disagree with the reviewer. The introduction in Part 1 is slightly long, but for a good reason – part of our goal is to convince the reader that such a new approach is needed. In other words, Section 1 of Part 1 is more than just an introduction; it also provides some of the key ideas we want to get across to the reader regarding the state of LSM development today and the unique role our new model can play. As for the introduction section in Part 2, the part that overlaps with Part 1 amounts to a single double-spaced page (at the beginning of the section), and the entire section amounts to about two double-spaced pages. We consider this to be concise enough to leave as is.

3. We now begin the sections on baseflow production and subsurface moisture transfer in Part 2 with relevant equations from Part 1, and we have added some sentences to the first paragraph of section 2.4.1 to emphasize how the discussion of the derivation of f in Part 2 complements the discussion of its use in Part 1. Hopefully, this will make Part 2 easier to read on its own.

4. We choose to keep sections 3.6-3.9 as they are. Section 3.6, which describes the ground thermodynamics, is already short (two paragraphs), and the information therein is not easily accessible in the literature. Our current revision of Section 3.7 is important when one considers the other reviewer's misinterpretation of the model's treatment of infiltration excess overland flow – some discussion about runoff generation in the model is definitely necessary. Section 3.8 describes baseflow and is very short as is. Finally, section 3.9 essentially describes specific revisions to the referenced snow model that were necessary for its incorporation into the catchment model.

5A. Scaling issues and data availability certainly do affect the believability of the model. We address these issues in a new paragraph, the second paragraph of section 2.6. As for showing how the test in Figure 6 applies to different watersheds, we already say that the success in that test is typical. Demonstrating this with more watersheds means generating more figures of the same sort, and we don't feel that the text strongly benefits from this. The scaling issues the reviewer hints at wouldn't show up anyway, since we don't apply any scaling functions to the soil parameters, and we apply a single scaling function to all topographic index means. In other words, a large watershed and a small one would behave the same if they had the same pdf of topographic index (and same vegetation, etc.)

5B. The moisture deficit is never low enough in this simulation – the catchments are never wet enough – for this source of bias to come into play. Instead, the apparent bias occurs when precipitation or net radiation rates are very low, so that differences in the normalized fluxes reflect very small errors. This is stated more clearly now in the second paragraph of section 4.1.

5C. The nature of the RMSE calculation – and how it relates to typical baseflow rates – is now clarified in the first paragraph of section 2.6.1.

6. We no longer say that the errors are of the same order as the observational error and instead give (general) reasons for why the discrepancy occurs. (See 2nd paragraph of section 4.1.) We point out that all of the PILPS models have the same basic problem.

A Catchment-Based Approach to Modeling Land Surface Processes in a GCM. Part 1: Model Structure

Randal D. Koster[1], Max J. Suarez[2], Agnès Ducharne[3], Marc Stieglitz[4], and Praveen Kumar[5]

May 10, 2000

[1]Hydrological Sciences Branch, Laboratory for Hydrospheric Processes, NASA/ Goddard Space Flight Center, Greenbelt, MD, USA.

[2]Climate and Radiation Branch, Laboratory for Atmospheres, NASA/Goddard Space Flight Center, Greenbelt, MD, USA.

[3]UMR, Sisyphe, UPMC Boite 123, 75251 Paris, France.

[4]Lamont-Doherty Earth Observatory, Columbia University, Palisades, NY, USA.

[5]Dept. of Civil Engineering, University of Illinois, Urbana-Champaign, Illinois, USA.

Abstract

A new strategy for modeling the land surface component of the climate system is described. The strategy is motivated by an arguable deficiency in most state-of-the-art land surface models (LSMs), namely the disproportionately higher emphasis given to the formulation of one-dimensional, vertical physics relative to the treatment of horizontal heterogeneity in surface properties — particularly subgrid soil moisture variability and its effects on runoff generation. The new strategy calls for the partitioning of the continental surface into a mosaic of hydrologic catchments, delineated through analysis of high-resolution surface elevation data. The effective "grid" used for the land surface is therefore not specified by the overlying atmospheric grid. Within each catchment, the variability of soil moisture is related to characteristics of the topography and to three bulk soil moisture variables through a well-established model of catchment processes. This modeled variability allows the partitioning of the catchment into several areas representing distinct hydrological regimes, wherein distinct (regime-specific) evaporation and runoff parameterizations are applied. Care is taken to ensure that the deficiencies of the catchment model in regions of little to moderate topography are minimized.

1 Introduction

1.1 History of LSM Development

Atmospheric general circulation models (GCMs) are invaluable tools for examining the mechanisms behind climate variability and for characterizing the sensitivity of climate to anthropogenic forcing. Of course, to be of value, a GCM must produce a realistic climate, and this requires realistic representations of the relevant physical processes. Over continents in particular, a proper representation of the land surface energy and water balance is critical. The land surface model (LSM) used with the GCM must, for example, properly partition the net incoming radiative energy into latent heat flux, sensible heat flux, ground heating, and snowmelt energy, and it must properly partition the precipitation at the surface into evaporation, runoff, and moisture storage. Complicating the development of an LSM is the inability, given current computer resources, to resolve explicitly the small-scale structure of the physical features that control these partitionings.

LSMs over the years have varied greatly in structure and complexity. In the simplest (and earliest) LSMs, land surface moisture conditions are prescribed — dry conditions are artificially maintained in deserts, for example, and wet conditions are maintained in tropical forests. This prescription has the advantage of ensuring reasonable evaporation fluxes across the globe, but it has the distinct disadvantage of precluding important land-atmosphere feedbacks, some of which lie at the heart of continental climate sensitivity.

This shortcoming is overcome by "interactive" land surface models. The simplest is the so-called "bucket" model of *Manabe et al.* [1969], which allows the water level in a soil moisture reservoir to increase during precipitation events and to decrease as the water evaporates. Because the evaporation efficiency varies with the water level in the reservoir, rainy periods lead to high evaporation rates, and droughts lead to low rates. Runoff occurs only when the soil moisture content exceeds field capacity. Manabe's original model has been adapted over the years to include, for example, multiple soil layers (*e.g., Hansen et al.* [1983]) and runoff generation from drier soils (*e.g., Gates and Schlesinger*, [1977]).

The "SVAT" (soil-vegetation-atmosphere transfer) model, a fundamentally different type of LSM, was introduced in the mid-1980's by *Sellers et al.* [1986] and *Dickinson et al.* [1986]. The SVAT approach gives vegetation a more direct role in determining the surface energy and water balance, particularly by allowing stomatal conductance to decrease in response to increased environmental stress. The evaporation formulation in most SVAT schemes can be described with the aid of a resistance diagram, and in the simpler SVAT schemes, this resistance diagram is equivalent to that of the Penman-Monteith evaporation formulation [*Monteith*, 1965]. The effects of vegetation on momentum transfer and on the surface radiation balance are also parameterized.

The roster of models used by participants in a recent major international intercomparison project (the Project for the Intercomparison of Landsurface Parameterizations Schemes, or PILPS) [*Henderson Sellers et al.*, 1993] indicates that the basic SVAT approach is the most popular and can, at least in that one sense, be considered the "state of the art". Numerous SVAT variations have been devised; for example, one recent PILPS experiment [*Chen et al.*, 1997] featured about twenty different SVAT LSMs. With some modeling groups, the SVAT approach is being enhanced by the inclusion of photosynthesis-transpiration physics [*Sellers et al.*, 1996; *Dickinson et al.*, 1998] and by a treatment of dynamic vegetation [*Foley et al.*, 1996; *Dickinson et al.*, 1998].

Of particular relevance for this paper are a few recent approaches that include an explicit representation of subgrid heterogeneity in surface characteristics. "Statistical-dynamical" approaches relate the surface energy and water fluxes to the spatial heterogeneity of the land surface and the meteorological forcing, characterized statistically [*e.g., Entekhabi and Eagleson*, 1989; *Famiglietti and Wood*, 1990; *Avissar*, 1992]. The "mosaic" approach involves separating the land surface grid element into subgrid tiles based on surface characteristics and then treating each tile separately in the simulation (*e.g., Avissar and Pielke* [1989], *Koster and Suarez* [1992], *Ducoudré et al.*, [1993], *Seth et al.* [1994]). A few LSMs have been built around relationships between topography and the subgrid variability of hydrological processes [*Famiglietti and Wood*, 1991, 1994; *Quinn et al.*, 1995a; *Stieglitz et* *al.*, 1997; *Liang et al.*, 1994]. As explained in the next section, we consider such a focus on subgrid variability to be critical to the realistic operation of an LSM.

1.2 Motivation for a New Strategy

PILPS [*Henderson-Sellers et al.*, 1993] was designed to document similarities and differences in the behaviors of the various state-of-the-art land surface models (LSMs) used with numerical atmospheric models. The main finding from PILPS was a wide disparity in LSM behavior in a number of environments [*Pitman et al.*, 1993; *Chen et al.*, 1997; *Wood et al.*, 1998]. The LSMs strongly disagree on how best to simulate land surface energy and water fluxes.

Koster and Milly [1997] addressed these differences with a focused study of LSM evaporation and runoff formulations. They avoided comparing specific details of the formulations, since an adequately thorough study of this type would be unmanageable. Rather, they focused on comparing the underlying, effective relationships that control the surface fluxes in the various PILPS LSMs. In particular, they examined the effective functional relationships between root zone soil moisture and both evaporation and runoff in each model. They found that the annual water balance is largely controlled by the shapes of these functional relationships and, in particular, by how these relationships are "positioned" relative to each other when plotted in the same figure. The upshot of their analysis is that annual evaporation rates are controlled as much by an LSM's runoff formulation as by its evaporation formulation. If the formulation of runoff in an LSM is poor, the LSM will produce unrealistic annual evaporation rates regardless of the quality of the evaporation formulation.

This result may seem obvious, but in some ways it is at odds with the apparent development strategies of many modeling groups. The evaporation and runoff formulations in LSMs are rarely of similar complexity — evaporation is usually given much more attention. Standard SVAT models account explicitly for canopy interception and for environmental influences (e.g., soil moisture availability, air temperature, vapor pressure deficit) on canopy conductance, using functions that can be quite complex. In addition, as mentioned earlier, a recent trend in model development is focusing on explicit treatments of photosynthic controls over transpiration and carbon uptake, and work is progressing in the dynamic prediction of vegetation phenology. The one-dimensional nature of the SVAT modeling approach encourages these modeling trends by allowing a detailed description of vertical canopy structure, a framework that is quite adequate for a first-order treatment of the essential biological processes involved in transpiration.

The one-dimensional framework, however, is not amenable to an adequate treatment of runoff generation, since runoff in nature is largely controlled by spatial heterogeneity in precipitation and surface conditions. Spatial heterogeneity in soil moisture is especially critical. Overland flow by the Dunne mechanism requires rainfall to impinge on a saturated ground surface, typically a small fraction of the land area receiving the rain. Overland flow by the Horton mechanism is generated when rainfall rate exceeds the infiltration capacity of the soil, and this infiltration capacity varies considerably in space with both soil texture and water content. Baseflow into rivers and streams reflects the three-dimensional structure of the water table. Given this complexity, an LSM that relies solely on a one-dimensional soil column for its hydrological calculations cannot hope to capture the main physical controls on runoff production. Thus, typical LSM runoff parameterizations, though given some attention over the years [*e.g., Entekhabi and Eagleson*, 1989; *Ducharne et al.*, 1998], are arguably crude in comparison to typical evaporation formulations.

This deficiency suggests a logical development path, namely, an improved treatment of the subgrid horizontal structure of land surface hydrological processes. We follow this path here. In our new LSM, subgrid heterogeneity in surface moisture state is treated statistically, since computational constraints (now and in the foreseeable future) prevent its explicit resolution. Nevertheless, the applied distributions are related sensibly to the topography, which exerts a major control over much of the subgrid variability. This representation of subgrid soil moisture variability allows, in principle, the explicit modeling of the runoff mechanisms outlined above. As an added benefit, it improves the representation of evaporation.

We describe our new LSM in sections 2 and 3 below; section 2 provides a broad overview of the modeling strategy, and section 3 provides specific details of the formulation. A discussion of the advantages of this modeling strategy follows in section 4.

The LSM has been fully coded and has been tested against observations. Details, along with a discussion of some unique parameter estimation issues, are provided in a companion paper [*Ducharne et al.*, this issue], hereafter referred to as Part 2.

2 The Catchment Model: Overall Framework

We now present a nontraditional land surface modeling framework that includes an explicit treatment of subgrid soil moisture variability and its effect on runoff and evaporation. Many of the ideas presented here and in the next section, which describes specific features of the model, are culled from works in the literature that have already recognized the importance of these issues. These works include those of *Famiglietti and Wood* [1991, 1994], who pioneered the idea of adding an energy balance to the TOPMODEL formalism [*Beven and Kirkby*, 1979; *Beven et al .*,, 1994; *Sivapalan et al.*, 1987] and applying the resulting LSM to each grid cell of a GCM, *Stieglitz et al.* [1997], who described a computationally efficient method of applying TOPMODEL equations to the land surface component of a GCM, and *Liang et al.* [1994], whose VIC model accounts explicitly for subgrid variability in infiltration capacity. The macroscale TOPLATS model of *Famiglietti and Wood* [1994] is indeed similar in concept to the present model in many ways. The two models differ significantly in many respects, though, such as in the interpretation of soil moisture distribution functions (see section 3.4) and in the variables used to describe soil moisture content above the water table.

Our description of the model's overall strategy divides itself naturally into two parts: (*i*) a description of the land surface element used and its connection to the overlying GCM atmospheric grid, and (*ii*) a description of the treatment of soil moisture variability within the element.

2.1 Partitioning of Continental Surfaces into Catchments

A key innovation in our approach involves the shape of the land surface element. We abandon the traditional approach of defining quasi-rectangular land surface elements with boundaries defined by the overlying atmospheric grid. Instead, we define the fundamental land surface element to be the hydrological catchment, with boundaries defined by topography.

Catchment boundaries have already been established over North America through the application of a geographical information system to a 30-arc-second resolution (approximately 1 kilometer) digital elevation model (DEM) provided by the U.S. Geological Survey. The catchment delineation in southwestern North America, for example, is shown in Figure 1. The delineation procedure considered network topology and drainage area [*Verdin and Jen-*

son, 1996; *Verdin and Verdin*, 1999] along with the application of ordering rules associated with a catchment coding system.

The average size of the catchments in North America is 3640 km^2. Thus, for a GCM run at a $4°\times5°$ resolution, which in midlatitudes is roughly equivalent to a grid cell of size 200000 km^2, the breakdown of the continent into catchments represents a significant degree of added resolution at the surface. Two catchments lying below the same atmospheric grid cell can be distinct in terms of the topographical parameters that describe soil moisture distributions (see below) and the vegetation type assumed for the catchment, which can be extracted from high resolution vegetation data sets [*DeFries*, 1994].

The mismatch between the regular atmospheric grid and the irregular catchment grid makes necessary an algorithm that disaggregates the atmospheric forcing to the catchment scale and aggregates the catchment "products" (*i.e.*, the surface turbulent, radiative, and momentum fluxes) to the GCM grid scale. For the aggregation of surface or near-surface fluxes onto the atmospheric grid, we use a conservative areal weighting scheme. The net flux, F_i, into atmospheric grid cell i is computed with

$$F_i = \frac{\Sigma_n F_n A_{ni}}{\Sigma_n A_{ni}}, \tag{1}$$

where A_{ni} is the area of catchment n that lies within the area defined by grid cell i. For the transformation of radiative fluxes and precipitation defined on the atmospheric grid onto the catchment grid, we use (in the present incarnation of the model) the analogous conservative scheme:

$$F_n = \frac{\Sigma_i F_i A_{ni}}{\Sigma_i A_{ni}}. \tag{2}$$

We currently apply (2) to the atmospheric state variables as well.

Of course, the coupling between the land and atmospheric models can (and should) be made more complex than this. Sub-gridscale variations in surface temperature and turbulent fluxes can, in principle, have important effects on the development of the boundary layer and on the generation of mesoscale circulations. Such inferred patterns, and variations in the topography itself, can in turn be incorporated into the disaggregation of the GCM forcing. Various disaggregation methods [*e.g., Gao and Sorooshian*, 1994; *Leung and Ghan*, 1995] are available in the literature and will eventually be incorporated into our overall approach. A full discussion of coupling issues is reserved for a future paper.

2.2 Subgrid Variability Within Each Catchment

As mentioned above, the separation of the continental surface into catchment elements allows for an explicit treatment of subgrid-scale heterogeneity at the land surface. Our strategy goes much further in this regard, though, because soil moisture is assumed to vary significantly within each catchment element. This is made straightforward by the use of a pre-existing, well-tested model of catchment processes, namely, TOPMODEL of *Beven and Kirkby* [1979]. We use this model to diagnose root zone soil moisture distributions from the morphology of the catchment and from our bulk soil moisture prognostic variables. (Note that alternative catchment hydrology models are also available, and some may be superior to TOPMODEL for describing many situations. As our catchment model evolves, we may choose to replace the TOPMODEL component with one of these alternatives. In other words, our overall framework is flexible; the use of TOPMODEL is simply considered a suitable starting point toward a proper representation of subgrid soil moisture variability. This is discussed further in section 4.1.)

The derived distribution of soil moisture in the root zone allows the separation of the catchment into specific hydrological regimes. Specifically, we derive: (*i*) the fraction of the catchment over which the ground surface is completely saturated (e.g., along riverbeds), (*ii*) the fraction of the catchment over which the ground surface is not saturated but transpiration nevertheless proceeds at the unstressed rate, and (*iii*) the fraction of the catchment over which the soil is too dry to allow any transpiration (i.e., the soil moisture is at or below the wilting point). This separation is the catchment strategy's most important advantage over the traditional one-dimensional SVAT model. The physical processes controlling runoff and evaporation are very different in these different regimes. Thus, the explicit partitioning of the catchment into the different areas and the application of different parameterizations in each area should lead to more credible estimates of evaporation and runoff across the catchment.

For example, the catchment LSM shuts off transpiration in the wilting fraction and computes unstressed transpiration in the other two fractions. Bare soil evaporation naturally proceeds at a very high rate in the saturated fraction, at a moderate rate in the unstressed fraction, and at a low rate in the wilting fraction. Infiltration and soil moisture diffusion effectively proceed at different rates in the different areas. Also, as in *Stieglitz et al.* [1997], we convert all precipitation into overland runoff in the saturated fraction of the catchment and allow part of the precipitation to infiltrate the soil in the other fractions. The water table distribution associated with the soil moisture distribution allows a physically-based calculation of baseflow.

At each time step, the surface water and energy fluxes computed for each areal fraction are combined into a single catchment flux, and the fluxes from adjoining catchments are then combined via (1) for input into the GCM. The areal fractions within a catchment, of course, respond dynamically to changes in the bulk water variables. Thus, the saturated fraction can grow and the wilting fraction might disappear during pluvial periods, and the reverse may occur during extended dry periods. The strength of these variations depends in large part on the topography. Given that we allow such dynamic changes in areal fraction, care is taken to ensure energy and water conservation across the catchment at all times.

3 The Catchment Model: Specific Details

3.1 The TOPMODEL Framework

Again, in its first incarnation, our LSM uses TOPMODEL equations to relate the water table distribution to the topography. (TOPMODEL in this paper refers to the original formulation of *Beven and Kirkby* [1979] and not to the fully developed LSM of *Beven et al.* [1994].) The TOPMODEL formulation [*Beven and Kirkby*, 1979; *Beven*, 1986a,b; *Sivapalan et al.*, 1987] allows a dynamically consistent calculation of the spatial distribution of water table depth in a catchment from knowledge of topography statistics. At the heart of TOPMODEL are three basic assumptions: (*i*) the water table is nearly parallel to the soil surface so that the local hydraulic gradient is close to tan β, where β is the local slope angle; (*ii*) the saturated hydraulic conductivity falls off exponentially with depth; and (*iii*) the water table is recharged at a spatially uniform, steady rate that is slow enough (relative to the response time of the catchment) to allow the assumption of a water table distribution that is always at equilibrium. Given these assumptions, an analytic relation can be derived between the catchment mean water table depth, $\overline{d}$, and the local water table depth, d, at an interior point:

$$d = \overline{d} - \frac{1}{\nu}\left(\ln\frac{a}{\tan\beta} - \overline{x}\right), \tag{3}$$

where $\ln(a/\tan\beta)$ is the "topographic index" at the point in question and $\overline{x}$ is the mean catchment value of the topographic index. The term a is the upstream area that contributes flow through a unit contour positioned at the point, and ν is the parameter describing the vertical profile of saturated hydraulic conductivity.

This framework by itself provides a method for calculating, from a single bulk moisture variable, the saturated areal fraction of the catchment (section 3.2) and the baseflow from the catchment. It cannot provide everything, however. In particular, because it focuses on equilibrium conditions for the water table, it does not address non-equilibrium moisture conditions in the vadose zone. Such non-equilibrium conditions are common and are critically important in the root zone, for example. Thus, the basic TOPMODEL framework is amended, as described below.

The distribution of topographic indices within a catchment can be extracted directly from digital elevation models (DEMs). Proper consideration must be given to the effects of DEM resolution on the character of the resulting distribution [*Wolock and McCabe* 1995; *Quinn et al.*, 1995b; *Wolock and Price*, 1994; *Zhang and Montgomery*, 1994], as discussed further in Part 2 [*Ducharne et al.*, this issue].

3.2 Soil Moisture Prognostic Variables

3.2.1 Catchment Deficit

The first bulk variable in our TOPMODEL-based catchment model is the "catchment deficit", M_D. The catchment deficit is defined as the average amount of water, per unit area, that would have to be added to bring all of the soil throughout the catchment to saturation, assuming that the unsaturated zone is initially in an equilibrium state.

This is a rather unconventional prognostic variable, and it thus deserves additional explanation. Figure 2 outlines the calculation of M_D. The top part of the figure shows the equilibrium profile of soil moisture with depth at an arbitrary point in the catchment. The part of the profile above the water table is determined from the balance between the pressure head gradient, which tends to draw moisture up, and gravity. The precise form of the equilibrium profile, as derived from the relations of *Clapp and Hornberger* [1978], is

$$w(z) = \left(\frac{\psi_s - z}{\psi_s} \right)^{-\frac{1}{b}}, \tag{4}$$

where w is the degree of saturation (or "wetness") at a height z above the water table, ψ_s is the matric potential in the soil at saturation, and b is a soil parameter. By vertically integrating $1 - w(z)$ over the unsaturated zone, we can determine the local moisture deficit, i.e., the amount of water that would need to be added at that point to bring the soil column to complete saturation.

The bottom part of Figure 2 illustrates the intuitive notion that the local moisture deficit varies significantly across the catchment, with low values where the water table is near the surface (at the bottom of hills) and high values where the water table is deeper (at the top of hills). Given an analytical distribution of the topographic index, the TOPMODEL equations provide an analytical distribution of water table depth in the catchment, from which an analytical distribution of local deficit can be readily derived. The catchment deficit can then be calculated as the integral of this local deficit across the catchment's area.

Note that this is a somewhat unusual (though not novel) application of the TOPMODEL framework. The TOPMODEL equations are not designed to generate soil moisture contents in the unsaturated zone and are not derived, in any case, from an assumption of equilibrium conditions above the water table. We simply use the TOPMODEL equations to describe the shape of the water table at any given time and then apply the equilibrium conditions as a straightforward way of characterizing, to first order, the moisture content above it. The combination of the TOPMODEL water table assumptions with the assumption of equilibrium moisture profiles allows a given value of catchment deficit to be associated with a unique description of equilibrium horizontal soil moisture variability.

To eliminate an unrealistic drift in the moisture state variables during extended dry periods, the model imposes a maximum catchment deficit based on estimated soil profile depths [*e.g., Webb et al.*, 1993]. The implications of this maximum value on the calculation of subgrid moisture regimes is discussed in section 3.4.

3.2.2 Root Zone Excess

If equilibrium conditions could indeed be assumed in the unsaturated zone, the catchment deficit by itself would be sufficient to characterize the catchment's complete moisture state — no other moisture variable would be needed. Equilibrium conditions, however, are generally not the rule. Soil moisture near the surface (*e.g.*, in the root zone) responds relatively quickly both to the infiltration of precipitation water and to the extraction of water via evapotranspiration. Given the critical role played by root zone moisture in the surface energy and water balances, we require a moisture variable that accounts for such non-equilibrium behavior. For this reason, we introduce the "root zone excess".

The root zone excess at a given point is defined as the amount by which the moisture in the root zone there exceeds (or is less than) the moisture content implied by the local equilibrium moisture profile. A positive point root zone excess is indicated by the lightly shaded area in Figure 3. The value becomes negative, of course, if evaporation exceeds precipitation over an extended period of time.

The point root zone excesses need not be the same throughout the catchment. The positive excesses that tend to follow a large storm, for example, cannot be realized in the areal fraction of the catchment that, at equilibrium, is already saturated. Nevertheless, our formulation uses a single, "bulk" root zone excess variable that represents the areal integral of the point excesses across the catchment. In other words, the root zone excess for the catchment, M_{RZ}, is the average amount of water, per unit area, by which conditions in the root zone across the catchment are out of equilibrium. The subcatchment distribution of point root zone excess is diagnosed from the bulk value through considerations of topography, vegetation, and other catchment features.

Combining the diagnosed distribution of point root zone excess with the distribution of equilibrium root zone moisture (as diagnosed from the catchment deficit) produces a distribution of total root zone moisture. This distribution is used to partition the catchment into subregions, as described in section 3.4.

3.2.3 Surface Excess

The third soil moisture prognostic variable is akin to the "surface soil layer" employed by many one-dimensional SVAT models. The "surface excess", M_{se}, essentially describes the degree to which the water in the top several centimeters of soil is out of equilbrium with the water in the root zone below it. A given catchment deficit and root zone excess uniquely define a distribution of root zone soil moisture, which in turn, through application of (4), can be used to diagnose a corresponding equilibrium distribution of surface moisture. The surface excess is defined as the average amount of water (per unit area) by which the actual surface moisture exceeds this equilibrium amount.

A positive surface excess is induced by the infiltration of rainwater or snowmelt, and a negative surface excess is induced by evaporation from the soil surface. The presence of this surface moisture variable was found to be crucial to an adequate treatment of bare soil evaporation and surface runoff generation.

Because the surface excess is assumed not to vary in space, the value for the catchment as a whole (i.e., the actual prognostic variable) is the same as that assumed for any local point. The total surface moisture nevertheless varies in space due to the topographically-induced variations in equilibrium soil moisture — the surface soil at the top of the hillslope will be drier than that on the valley floor. If the assumption of uniformity leads to any local impossibilities in moisture content, such as moistures in excess of saturation, the catchment value of surface excess is adjusted accordingly.

3.3 Transfers Between Moisture Reservoirs

3.3.1 Transfer Between the Root Zone and the Water Table

The root zone excess continually interacts with the equilibrium water state. If the root zone excess is positive, some water is transferred from the root zone to the equilibrium state, and the water table rises. Alternatively, if the excess is negative, the root zone gains some water and the water table falls. Thus, this interaction, applied at each simulation timestep, always acts to reduce the absolute magnitude of the excess — it always acts to bring the total system closer to equilibrium conditions.

The calculation of this moisture transfer, ΔM, takes advantage of the subcatchment soil moisture distributions diagnosed from the two bulk moisture variables and the topographic characteristics. To see how this is done, consider first a somewhat impractical approach. The catchment is separated into a multitude of small pixels. At each pixel, the local root zone excess and depth to the water table is established from the subcatchment distributions, and the Richards equation is solved (over a highly resolved discretization of the vertical moisture profile) to approximate the local transfer between the excess and the underlying equilibrium profile. The pixel-based transfers are then summed across the catchment to produce ΔM, which is then used to update the two bulk variables.

The impracticality of this distributed approach stems from its high computational expense. The conceptual advantages of a distributed calculation, however, can nevertheless be captured by a much simpler formulation. We perform, prior to any climate simulation, detailed distributed calculations in a given catchment over a wide range of M_D and M_{RZ} values. The results are processed into a simple, approximate catchment-specific relationship between ΔM, M_D, and M_{RZ}, having the following form:

$$\Delta M_{\mathrm{rz}} = -M_{\mathrm{rz}} \frac{\Delta t}{\tau_1} \tag{5}$$

and

$$\Delta M_{\mathrm{D}} = -M_{\mathrm{rz}} \frac{\Delta t}{\tau_1}, \tag{6}$$

where Δt is the the timestep length and τ_1 is a timescale of moisture transfer, an empirical function of M_D and M_{RZ}. The precise form of this empirical function, as derived from the distributed calculations, is described in Part 2 [*Ducharne et al.*, this issue]. In essence, τ_1 decreases with decreasing M_D and with increasing M_{RZ}. Its sensitivity to these bulk variables varies with topography and thus varies from catchment to catchment.

3.3.2 Transfer Between Surface Excess and Root Zone Excess

The magnitude of the surface excess, M_{se}, is reduced at every timestep through the transfer of moisture between the surface excess and root zone excess variables:

$$\Delta M_{\mathrm{se}} = -M_{\mathrm{se}} \frac{\Delta t}{\tau_2}, \tag{7}$$

and

$$\Delta M_{\mathrm{rz}} = M_{\mathrm{se}} \frac{\Delta t}{\tau_2}, \tag{8}$$

where τ_2 is a timescale analogous to τ_1 in (5) and (6). The value of τ_2 decreases with an increase in either the total root zone moisture or the surface excess. The form of the empirical function used for τ_2 is presented in Part 2 [*Ducharne et al.*, this issue].

3.4 Spatial Partitioning Within the Catchment

The bulk moisture variables allow the catchment to be separated into three distinct regions. The "saturated region" consists of all points for which the root zone is fully saturated, and it has a fractional area of A_{sat}. The "transpiration" region, consisting of all points having subsaturated root zone moistures that lie above the vegetation-specific wilting point (θ_{wilt}), has a fractional area of A_{tr}. Finally, the "wilting" region, consisting of all points for which transpiration is shut off completely, has a fractional area of A_{wilt}.

The areal fractions are determined through manipulation of a derived probability density function (pdf) of root zone soil moisture. If the water table lies above the assumed bedrock depth, then associated with each point in the catchment is a specific equilibrium moisture profile, represented by (4). Integrating this vertical profile across the root zone alone gives a local equilibrium root zone moisture, m_{rz}:

$$m_{\mathrm{rz}} = \frac{1}{d_{\mathrm{rz}}} \int_{\overline{d}-d_{\mathrm{rz}}}^{\overline{d}} w(z) dz, \tag{9}$$

where d_{rz} is the depth of the root zone. Equations (4) and (9) allow us to transform the pdf of water table depth into a pdf of equilibrium root zone moisture across the catchment. This pdf has a complex form that is nevertheless amenable to a simple approximate representation, as described in Part 2 [*Ducharne et al.*, this issue]. A typical shape of this pdf is shown in Figure 4 by curve (A); the pdf is characterized in part by a minimum soil moisture, θ_0.

Again, the pdf described above is for the equilibrium soil wetness. If the water table depth corresponding to the current catchment deficit, however, lies below the assumed bedrock depth, then no free-standing water table is assumed to exist in the catchment, and the determination of the "equilibrium" pdf (still defined as the pdf associated with the current value of M_D) must be revised. This is done by assuming specific shapes for the pdfs at three critical values of M_D. These shapes are indicated by the curves (B), (C), and (D) in Figure 4. The first pdf, (B), corresponds to the point at which the mean water table depth is exactly the assumed depth to bedrock; this is taken to be the last point at which an assumed water table can influence the shape of the root zone wetness pdf. The second pdf, (C), corresponds to the onset of wilting ($\theta_0 = \theta_{\text{wilt}}$). The shapes of (B) and (C) are the same because prior to wilting, the main sink of moisture, evapotranspiration, is assumed for convenience to act uniformly on the root zone moisture — unstressed transpiration does take place, after all, in both the saturated and transpiration fractions. Thus, the soil in the non-wilting catchment is assumed to dry uniformly, leading to a simple translation of the pdf. (Note that with the bedrock depths we assume, which are consistent with the bedrock depths typically assumed implicitly by TOPMODEL, the relative positions of (B) and (C) are always maintained, i.e., at state (B), the soil moisture everywhere lies above the wilting point.) The final pdf we consider, (D), corresponds to complete wilting and is represented by a simple delta function centered at θ_{wilt}.

The values for A_{sat}, A_{tr}, and A_{wilt} vary according to where M_D and the current value of the root zone excess, M_{rz}, position the "non-equilibrium" pdf of soil moisture (i.e., the pdf corrected for root zone excess) in Figure 4. M_{rz} basically acts to translate along the θ axis the pdf established by M_D. Details are presented in Appendix A.

Again, the separation of the catchment into the three subregions constitutes a critical advantage of the catchment model. The physical mechanisms that control evaporation and runoff generation in these subregions are fundamentally different. The explicit separation of the subregions allows us to employ the appropriate treatments in each.

Such manipulation of pdfs, by the way, distinguish this LSM from some other topography-based LSMs, such as TOPLATS [*Famiglietti and Wood*, 1994] and the model of *Quinn et al.* [1995b]. In these other models, the pdf of topographic index itself is discretized, and calculations are performed over each pdf interval. In the catchment LSM described here, the analytical topographic index distribution is effectively transformed into an analytical distribution of root zone moisture, which in turn is discretized into at most three hydrological regimes of relevance.

3.5 Surface Energy Balance Calculations

Full details of the energy balance calculations are not provided here, since they parallel exactly those in the Mosaic LSM of *Koster and Suarez* [1992, 1996]. We focus instead on those aspects of the calculations that are unique to the catchment model. In effect, a full one-dimensional SVAT model computes the energy balance separately in each of the three subregions. In accordance with the modeled distribution of soil moisture, the resistances applied to the evapotranspiration calculation (a critical component of the energy balance calculation) vary significantly between the subregions. For example, resistance to bare soil evaporation, a function of surface soil moisture [*Koster and Suarez*, 1996], is very small in the saturated region, is moderate in the transpiration region, and is high in the wilting region. The same small but nonzero resistance (a function of vegetation type, solar radiation, and ambient air temperature) limits transpiration in both the saturated and transpiration subregions, whereas in the wilting region, this resistance is set high enough to shut down transpiration completely.

Each subregion maintains its own prognostic surface temperature; no "smoothing out" of this temperature is performed at the end of a time step. This allows the valley bottoms, where more evapotranspiration occurs, to remain consistently cooler than the drier hilltops.

Note that an intermediate "moisture-stressed" evaporation regime is not included in this formulation — transpiration proceeds at an unstressed rate in the two wetter subregions and does not occur at all in the driest subregion. We neglect moisture-stressed nonzero transpiration for two reasons. First, the moisture regime over which it occurs is relatively small; once plants begin to be moisture-stressed, only a small additional amount of drying leads to total wilting. By ignoring this small regime, we can avoid the application of a complex moisture-stressed transpiration model, which requires parameters that are very difficult to estimate. Second, a key reason for including moisture-stressed evaporation in many LSMs is to allow a smooth transition between the full transpiration and full wilting regimes. The catchment model achieves this smooth transition through the dynamically varying areas of the subregions.

3.6 Ground Thermodynamics

Although each of the three subregions maintains its own surface/canopy temperature, temperatures at deeper levels are assumed to be spatially homogeneous. Figure 5 illustrates the framework applied to the calculation of the ground temperatures. The net heat flux from layer 1 to layer 2 in the figure is computed by weighting the individual heat flux from each surface subregion by its respective area and then summing together the three weighted fluxes. Heat transport within the soil column is governed by linear diffusion along the thermal gradient. As indicated in the figure, layer thicknesses follow a geometric series. The top layer's thickness is taken to be 5 cm to allow us to capture the diurnal range in the surface radiating temperature. The ground profile extends to a depth of 10m to be compatible with the assumption that the bottom boundary of the deepest model layer is completely insulating; this depth is approximately three times the seasonal damping depth of typical soils.

Note that the thicknesses associated with the layers in Figure 5 are unrelated to the layer thicknesses associated with the moisture prognostic variables, being chosen instead for consistency with the heat diffusion calculations. Even so, heat conductivity does increase in a simple way with increasing bulk soil moisture.

3.7 Canopy Interception, Throughfall and Surface Runoff

A prognostic moisture variable not mentioned above is canopy interception, i.e., the easily evaporated water that sits on leaves and ground litter following rain events. A single interception reservoir overlies all three catchment subregions. Interception storage and evaporation is treated exactly as it is in the Mosaic LSM [*Koster and Suarez*, 1996]. The storage capacity is a simple function of leaf area index. A simple representation of subgrid storm position "memory" ensures that some of the precipitation (the "throughfall") will almost always fall through the canopy to the ground surface.

The throughfall, P_T, falls uniformly on all three catchment subregions. Throughfall impinging on the saturated region is immediately converted into surface runoff. Throughfall impinging on the other areas infiltrates the soil, unless the soil is frozen or the surface excess, M_{se}, is positive, indicating a rain-induced build-up of moisture near the surface. In the latter case, some overland flow, Q_s, is allowed from the transpiration area only. The full equation for overland flow is:

$$
\begin{aligned}
Q_s &= P_T A_{\mathrm{sat}} \qquad (M_{\mathrm{se}} < 0) \\
Q_s &= P_T \left(A_{\mathrm{sat}} + A_{\mathrm{tr}} \frac{M_{\mathrm{se}}}{M_{\mathrm{se-max}}} \right) \qquad (M_{\mathrm{se}} > 0)
\end{aligned}
\tag{10}
$$

In (10), $M_{\mathrm{se-max}}$ is the maximum possible value of the surface excess given the current values of catchment deficit and root zone excess. If infiltration saturates the surface layer, the excess over saturation is converted into surface runoff.

The quantity $P_T A_{\mathrm{tr}} M_{\mathrm{se}}/M_{\mathrm{se-max}}$ in (10) effectively represents infiltration excess overland flow. This term is designed to capture, in a crude way, a smooth transition between zero runoff production when the surface soil is relatively dry (M_{se} is zero or less) to a complete conversion of rainfall into runoff when heavy rains bring the moisture near the surface to its maximum value. This term represents an exceedance of the soil's "infiltration rate" in the sense that the timescale of moisture transfer from the surface layer to the root zone, τ_2 in (8), can be too large to maintain low M_{se} values during a rainstorm. Note that when the soil column is parched, water in the surface layer (and thus M_{se}) can build up relatively quickly due to its larger τ_2. Thus, even though it has a larger $M_{\mathrm{se-max}}$, a parched soil can be conducive to converting rainfall to overland flow.

3.8 Baseflow

The calculation of baseflow, or the loss of groundwater to streams, is straightforward given the use of TOPMODEL equations to describe the distribution of water table depth. The TOPMODEL framework [*Sivapalan et al.*, 1987] relates baseflow, G, directly to the mean water table depth, $\overline{d}$:

$$G = \frac{K_s(\text{surface})}{\nu} e^{-\overline{x}-\nu\overline{d}}. \tag{11}$$

Because the catchment deficit in a given catchment is a unique function of the mean water table depth, a simple relationship between baseflow and M_D can be easily derived. The particular relationship used is described in Part 2 [*Ducharne et al.*, this issue].

As discussed in section 3.4, a bedrock depth is assumed in the calculation of A_{sat}, A_{tr}, and A_{wilt}. Baseflow is shut off when $\overline{d}$ falls below this bedrock depth.

3.9 Snow Model

The snow model of *Lynch-Steiglitz* [1994] has been coupled to the catchment model. This three-layer snow model accounts for snow melting and refreezing, dynamic changes in snow density, snow insulating properties, and other physics relevant to the growth and ablation of the snowpack. It has been tested with considerable success against detailed measurements in the Sleepers River catchment of Vermont.

The catchment framework, however, necessitated some modifications to the original scheme. In particular, we now ensure a smooth transition between snow-free and snow-covered conditions in order to capture the gradual growth of a snowpack's spatial extent and to avoid abrupt changes in the surface energy balance calculations. The approach used is straightforward.

We assume a minimum local snow water equivalent of 13mm, a value that allows the resolution of the diurnal surface temperature signal yet still produces a stable solution with a 20-minute timestep. If a given volume of snow falls on a snow-free catchment, that volume is spread uniformly over a fraction of the catchment so that the local water equivalent at any snow-covered point is 13mm. Thus, if the snow falling in a timestep has a total (water-equivalent) volume V in m^3, and if the area of the catchment is A in m^2, then the snow-covered areal fraction, A_s/A, is taken to be

$$\frac{A_s}{A} = \frac{V}{.013A} \quad . \tag{12}$$

The snow-covered areal fraction increases similarly as more snow falls until it reaches 1, at which time the local water equivalents across the catchment start increasing uniformly.

Surface energy calculations are performed separately over the snow free and snow covered areas. When the fractional coverage is less than one, the snow model is represented with a single snow layer, whereas three model layers are used when the snow coverage is complete [*Lynch-Stieglitz*, 1994]. The transition between the single layer and three layer representations involves a simple conservative redistribution of layer heat and water contents.

A paper describing this snow model, its interaction with the simulated water balance of the catchment, and its validation against available observations is currently in preparation (Stieglitz, pers. comm.).

4 Discussion

4.1 TOPMODEL Limitations

Because the catchment model employs TOPMODEL equations, we must pay special attention to the behavior of the LSM in regions of low topography, where the advantages of TOPMODEL are lost. In the limiting case of perfectly flat terrain, topography-based variations in soil moisture are eliminated. The land surface element is therefore not areally partitioned into distinct moisture regimes. Furthermore, each point in the element has the same assumed moisture profile in the unsaturated zone and the same assumed depth to the water table. As a result, the formulation of subsurface moisture transport, which was described in section 3.3 as equivalent to an areal integration of distributed Richards equation solutions, reduces in the flat case to a single, one-dimensional application of the Richards equation. In the flat case, the LSM can therefore be considered equivalent to a traditional three-layer LSM — it uses the one-dimensional Richards equation to transport moisture between a surface moisture reservoir, a root zone reservoir, and an "equilibrium" reservoir that mainly reflects moisture conditions deeper in the soil.

A region's terrain, of course, is never perfectly level. As topographical variations decrease, however, the catchment LSM will capture more and more of the flavor of a traditional three-layer model. The use of the root zone and surface excess variables allows the catchment LSM to function at least as well as traditional LSMs in flatter areas, despite TOPMODEL's limitations there.

Other limitations of TOPMODEL must also be considered. Key among them is the assumption that the water table within a catchment is everywhere parallel to the ground surface, which is an oversimplification, especially at larger spatial scales. In fact, at such scales (several kilometers or more), subsurface flow may be controlled more by local geology and geomorphology. We nevertheless consider the use of TOPMODEL equations to be the appropriate first step in the direction away from the traditional one-dimensional "layer" approach to modeling subsurface soil moisture transport. It appears, in fact, to be the most sensible step to take at this time given the availability of global topographic data, the lack of other relevant data (e.g., bedrock depths) on the global scale, and the inability, in any case, to avoid a statistical characterization of subgrid moisture distributions under current computational constraints. TOPMODEL, though perhaps not optimal for the spatial scales we are considering, nevertheless captures the critical differences between upslope and downslope hydrological behavior and should give a useful first order description of subgrid soil moisture variability. This is, in fact, supported by the applications of the catchment LSM described in Part 2 [*Ducharne et al.*, this issue].

In any case, as mentioned before, the modeling framework is flexible, and like all LSMs, the catchment model will continue to evolve. We can certainly incorporate more realistic soil moisture characterizations into the model as they (and the supporting data) become available.

4.2 Additional Conceptual Advantages

A few additional advantages of the catchment approach should be mentioned. First, the partitioning of the continental surface into a mosaic of catchment "tiles" allows a straightforward calculation of annual streamflow from large river basins. The algorithms used to delineate catchment boundaries from digital elevation map data [*Verdin and Jenson*, 1996; *Verdin and Verdin*, 1999] establish flow directions and identify the set of catchments that lie within a given larger basin; the resulting annual streamflow for the larger basin can thus be calculated easily from the catchment values [*Ducharne et al.*, 1998]. This is important, of course, for model validation at the annual timescale and for the coupling of LSM runoff products to an ocean model. The catchment framework also supports the development and use of river routing schemes that emphasize the timing of river water transport, which is crucial for model validation at shorter timescales.

Second, the explicit treatment of subgrid soil moisture distributions is amenable to a more tenable validation of modeled soil moisture against observations. Such validation with traditional one-dimensional LSMs, though given some attention in recent years (*e.g., Robock et al.* [1995]), is conceptually limited by the nonlinear relationship between soil moisture and evaporation; given a realistic point evaporation function, a single (in the horizontal) moisture variable in a traditional layer-type LSM cannot produce a realistic average evaporation rate if it must also represent an areally-averaged soil moisture content. With the catchment LSM, realistic evaporation rates and soil moisture contents can theoretically coexist. In addition to model validation, of course, this has important implications for the potential assimilation of observed soil moisture data into the model.

Third, the framework is amenable to the elevation-based disaggregation of the grid-scale atmospheric forcing provided by the GCM. We can make use of the detailed topographical characterization of each catchment and its neighbors to assign, for example, lower near-surface atmospheric temperatures to higher elevation catchments or to the higher areas of an individual catchment. These elevation-based temperatures could lead to elevation-based variations in surface heat fluxes and snowmelt. Variations in shortwave radiation with topographical aspect could perhaps be included. Procedures for disaggregating precipitation by elevation already exist in the literature [*e.g., Leung and Ghan*, 1995].

Finally, and perhaps most importantly, the specification of the catchment as the fundamental land surface element provides a more direct link to basic hydrological science, for which the catchment is a natural unit of study. Our model development can take advantage of watershed studies that span several decades. The use of the TOPMODEL framework is considered a useful starting point in this development. Useful features of other catchment hydrology models can be incorporated into our new LSM as they are identified.

5 Summary

We have described a strategy for improving what appears to be a "weak link" in most land surface models (LSMs), namely the characterization of subgrid soil moisture variability and its impact on runoff generation. The catchment strategy differs from the traditional SVAT strategy in two important ways. First, the boundaries of the basic land surface element, the hydrological catchment, are derived from topographic data. They are thus irregular and independent of the overlying atmospheric grid. Second, subcatchment distributions of root zone soil moisture are diagnosed from bulk moisture variables and topographic characteristics. The distributions are used to divide the catchment's area into three sections, each representing a distinct moisture regime. Evaporation and runoff processes are modeled differently in each section, thereby producing a more credible estimate (at least in theory) of the catchment-mean rates.

The catchment LSM uses three non-traditional bulk moisture variables to describe the catchment moisture state, one representing equilibrium conditions associated with the water table distribution, and the others representing non-equilibrium conditions near the surface. The LSM currently uses the TOPMODEL formulation of *Beven and Kirkby* [1979] to establish the water table distribution. The limitations of TOPMODEL in low topography regions are diminished through the use of the non-equilibrium moisture variables — in low topography regions, the model reduces to a more traditional layer-type LSM.

The catchment strategy has several advantages. The two most important are: (*i*) the explicit treatment of subgrid soil moisture variability allows for more realistic formulations of evaporation and (especially) runoff; and (*ii*) the use of the catchment as the land surface element allows a strong connection between LSM structure and established hydrological models, which will be helpful in the future evolution of our LSM. The overall strategy, which builds on the work of others who have recognized the importance of the runoff formulation in LSMs [*Famiglietti and Wood*, 1991, 1994; *Liang et al.*, 1994; *Stieglitz et al.*, 1997], avoids many of the problems limiting standard representations of land surface processes.

Although the catchment strategy's conceptual advantages are important in themselves, the strength of the approach is best demonstrated through an application of the fully coded model in a real setting, with observed meteorological variables for forcing the model and observed water fluxes for evaluating the model's performance. Such an analysis is presented in Part 2 [*Ducharne et al.*, this issue].

Appendix A: Equations Used to Partition the Catchment

In the discussion below, the average equilibrium root zone moisture at states (A), (B), and (C) in Figure 4 will be referred to as $\overline{\theta_{(\mathrm{A})}}$, $\overline{\theta_{(\mathrm{B})}}$, and $\overline{\theta_{(\mathrm{C})}}$, the catchment deficits at states (A), (B), (C) and (D) will be referred to as M_D, $M^{(\mathrm{B})}$, $M^{(\mathrm{C})}$, and $M^{(\mathrm{D})}$, and the equilibrium pdfs at states (A), (B) and (C) will be referred to as $f(\theta)$, $f_{(\mathrm{B})}(\theta)$ and $f_{(\mathrm{C})}(\theta)$. The average root zone moisture at state (D) is, by definition, θ_{wilt}.

Also, a dimensionless root zone excess, θ_{exc}, is used below. It is computed by dividing the root zone excess prognostic variable, M_{rz}, by the water holding capacity of the root zone. The mean root zone wetness at a given time, corrected for the root zone excess, is thus $\theta_{(\mathrm{A})} + \theta_{\mathrm{exc}}$.

The equations for A_{sat}, A_{tr}, and A_{wilt} vary according to where M_D and θ_{exc} position the non-equilibrium pdf of soil moisture in Figure 4. If $M_{\mathrm{D}} < M^{(\mathrm{B})}$, so that a water table is active, and if the root zone excess does not bring any part of the pdf below the wilting point, then we compute

$$A_{\mathrm{sat}} = \int_1^{\infty} f(\theta - \theta_{\mathrm{exc}}) d\theta$$

$$A_{\mathrm{tr}} = 1. - A_{\mathrm{sat}}$$

$$A_{\mathrm{wilt}} = 0. \tag{13}$$

If $M_{\mathrm{D}} < M^{(\mathrm{B})}$ but the root zone excess does bring part of the pdf below the wilting point, we assume the wilting fraction to vary linearly between 0 (at

$\theta_{(\mathrm{A})} + \theta_{\mathrm{exc}} = \theta_{(\mathrm{C})}$) and 1 (at $\theta_{(\mathrm{A})} + \theta_{\mathrm{exc}} = \theta_{\mathrm{wilt}}$):

$$A_{\mathrm{wilt}} = \frac{\overline{\theta_{(\mathrm{C})}} - \overline{\theta_{(\mathrm{A})}} - \theta_{\mathrm{exc}}}{\overline{\theta_{(\mathrm{C})}} - \theta_{\mathrm{wilt}}}$$

$$A_{\mathrm{sat}} = (1 - A_{\mathrm{wilt}}) \int_1^{\infty} f(\theta - \theta_{\mathrm{exc}}) d\theta$$

$$A_{\mathrm{tr}} = 1. - A_{\mathrm{sat}} - A_{\mathrm{wilt}}. \qquad (14)$$

If $M_{\mathrm{D}} > M^{(\mathrm{B})}$, then no water table is active, and the "equilibrium" average root zone moisture associated with M_D is computed assuming a linear variation of $\overline{\theta_{(\mathrm{A})}}$ with M_{D}:

$$\overline{\theta_{(\mathrm{A})}} = \theta_{\mathrm{wilt}} + \left(\overline{\theta_{(\mathrm{B})}} - \theta_{\mathrm{wilt}}\right) \frac{M^{(\mathrm{D})} - M_{\mathrm{D}}}{M^{(\mathrm{D})} - M^{(\mathrm{B})}}. \qquad (15)$$

Adding θ_{exc} to $\overline{\theta_{(\mathrm{A})}}$ in this "no water table" case will bring the average root zone moisture into one of three regimes. First, if $\overline{\theta_{(\mathrm{A})}} + \theta_{\mathrm{exc}} > \overline{\theta_{(\mathrm{B})}}$ (i.e., the average root zone moisture is above $\overline{\theta_{(\mathrm{B})}}$), the areas are computed with

$$A_{\mathrm{sat}} = \int_1^{\infty} f_{(\mathrm{B})}(\theta + \overline{\theta_{(\mathrm{B})}} - \overline{\theta_{(\mathrm{A})}} - \theta_{\mathrm{exc}}) d\theta$$

$$A_{\mathrm{tr}} = 1. - A_{\mathrm{sat}}$$

$$A_{\mathrm{wilt}} = 0. \qquad (16)$$

Second, if $\overline{\theta_{(\mathrm{C})}} < \overline{\theta_{(\mathrm{A})}} + \theta_{\mathrm{exc}} < \overline{\theta_{(\mathrm{B})}}$, then the final pdf lies between states (B) and (C), and the areas are calculated with

$$A_{\mathrm{sat}} = A_{\mathrm{sat}}^{(\mathrm{C})} + \frac{\overline{\theta_{(\mathrm{A})}} + \theta_{\mathrm{exc}} - \overline{\theta_{(\mathrm{C})}}}{\overline{\theta_{(\mathrm{B})}} - \overline{\theta_{(\mathrm{C})}}} \left(A_{\mathrm{sat}}^{(\mathrm{B})} - A_{\mathrm{sat}}^{(\mathrm{C})}\right)$$

$$A_{\mathrm{tr}} = 1. - A_{\mathrm{sat}}$$

$$A_{\text{wilt}} = 0, \tag{17}$$

where

$$A_{\text{sat}}^{(\text{B})} = \int_1^\infty f_{(\text{B})}(\theta)d\theta \tag{18}$$

and

$$A_{\text{sat}}^{(\text{C})} = \int_1^\infty f_{(\text{C})}(\theta)d\theta. \tag{19}$$

Finally, if $\overline{\theta_{(\text{A})}} + \theta_{\text{exc}} < \overline{\theta_{(\text{C})}}$, wilting occurs over a portion of the catchment. We compute:

$$A_{\text{wilt}} = \frac{\overline{\theta_{(\text{C})}} - \overline{\theta_{(\text{A})}} - \theta_{\text{exc}}}{\overline{\theta_{(\text{C})}} - \theta_{\text{wilt}}}$$

$$A_{\text{sat}} = A_{\text{sat}}^{(\text{C})}\left(1 - A_{\text{wilt}}\right)$$

$$A_{\text{tr}} = 1 - A_{\text{sat}} - A_{\text{wilt}}. \tag{20}$$

Acknowledgments. This work was supported by funding from the Earth Science Enterprise of NASA Headquarters through the EOS-Interdisciplinary Science Program and the NASA Seasonal-to-Interannual Prediction Project (NSIPP). Comments by three reviewers of an earlier draft were insightful and very helpful. Kris Verdin and the USGS EROS Data Center are thanked for their help with the processing of the topographic data.

References

Avissar, R., Conceptual aspects of a statistical-dynamical approach to represent landscape subgrid-scale heterogeneities in atmospheric models, *J. Geophys. Res.*, *97*, 2729-2742, 1992.

Avissar, R. and R. Pielke, A parameterization of heterogeneous land surfaces for atmospheric numerical models and its impact on regional meteorology, *Mon. Wea. Rev.*, *117*, 2113-2136, 1989.

Beven, K. R., and M. J. Kirkby, A physically-based variable contributing area model of basin hydrology, *Hydrol. Sci. J.*, *24*, 43-69, 1979.

Beven, K. R., Hillslope runoff processes and flood frequency characteristics, *Hillslope Processes*, A. D. Abrahams, Ed., Allen and Unwin, 187-202, 1986a.

Beven, K. R., Runoff production and flood frequency in catchments of order n, an alternative approach, *Scale Problems in Hydrology*, V.K. Gupta, I. Rodriguez-Iturbe, and E. F. Wood, Eds., D. Reidel, 107-131, 1986b.

Beven, K. R., P. Quinn, R. Romanowicz, J. Freer, J. Fisher, and R. Lamb, TOPMODEL and GRIDATB, A users guide to the distribution versions (94.01), *Tech. Rep. TR110/94*, Centre for Res. on Environ. Syst. and Stat., Lancaster University, Lancaster, U.K., 1994.

Chen, T.H., A. Henderson-Sellers, P.C.D. Milly, A. J. Pitman, A.C.M Beljaars, and 38 others, Cabauw experimental results from the Project for Intercomparison of Landsurface Parameterization Schemes (PILPS), *J. Climate*, *10*, 1194-1215, 1997.

Clapp, R.B., and G.M. Hornberger, Empirical equations for some soil hydraulic properties, *Water Resour. Res.*, *14*, 601-604, 1978.

Cosby, B. J., G. M. Hornberger, R. B. Clapp, and T. R. Ginn, A statistical exploration of the relationships of soil moisture characteristics to the physical properties of soils, *Water Resour. Res.*, *20*, 682-690, 1984.

DeFries, R. S. and J. R. G. Townshend, NDVI-derived land cover classification at global scales, *Int. J. Rem. Sens.*, *15*, 3567-3586, 1994.

Dickinson, R. E., A. Henderson-Sellers, P. J. Kennedy, and M. F. Wilson, Biosphere - atmosphere transfer scheme (BATS) for the NCAR Community Climate Model, *Technical Note TN-275+STR*, National Center for Atmospheric Research, Boulder, CO, 69 pp., 1986.

Dickinson, R. E., M. Shaikh, R. Bryant, and L. Graumlich, Interactive canopies for a climate model, *J. Climate*, *11*, 2823-2836, 1998.

Ducharne, A., K. Laval, and J. Polcher, Sensitivity of the hydrological cycle to the parameterization of soil hydrology in a GCM, *Clim. Dyn.*, *14*, 307-327, 1998.

Ducharne, A., R. D. Koster, M. J. Suarez, and P. Kumar, A catchment-based land surface model for GCMs and the framework for its evaluation, *Physics and Chemistry of the Earth*, *24*, 769-773, 1998.

Ducoudré, N. I., K. Laval, and A. Perrier, SECHIBA, a new set of parameterizations of the hydrologic exchanges at the land/atmosphere interface within the LMD atmospheric general circulation model, *J. Climate*, *6*, 248-273, 1993.

Entekhabi, D. and P. Eagleson, Land surface hydrology parameterization for atmospheric general circulation models including subgrid scale spatial variability, *J. Climate*, *2*, 816-831, 1989.

Famiglietti, J. and E. Wood, Evapotranspiration and runoff from large land areas: land surface hydrology for atmospheric general circulation models, *Land Surface-Atmospheric Interactions for Climate Models: Observations, Models, and Analyses*, edited by E. Wood, pp. 179-204, Kluwer Academic Publishers, 1990.

Famiglietti, J., and E. Wood, Evapotranspiration and runoff from large land areas: Land surface hydrology for atmospheric general circulation models, *Surv. Geophysics*, *12*, 179-204, 1991.

Famiglietti, J., and E. Wood, Multiscale modeling of spatially variable water and energy balance processes, *Water Resources Research*, *30*, 3061-3078, 1994.

Foley, J. A., I. C. Prentice, N. Ramankutty, S. Levis, D. Pollard, S. Sitch, and A. Haxeltine, An integrated biosphere model of land surface processes, terrestrial carbon balance, and vegetation dynamics, *Global Biogeochemical Cycles*, *10*, 603-628, 1996.

Gao, X. G. and S. Sorooshian, A stochastic precipitation disaggregation scheme for GCM applications, *J. Climate*, *7*, 238-247, 1994.

Gates, W. L., and M. E. Schlesinger, Numerical simulation of the January and July global climate with a two-level atmospheric model, *J. Atmos. Sci.*, *34*, 36-76, 1977.

Hansen, J., G. Russell, D. Rind, P. Stone, A. Lacis, S. Lebedeff, R. Ruedy, and L. Travis, Efficient three-dimensional global models for climate studies: Models I and II, *Mon. Weather Rev.*, *111*, 609-662, 1983.

Henderson-Sellers, A., Z.-L. Yang, and R. E. Dickinson, The Project for Intercomparison of Land-surface Parameterization Schemes, *Bull. Am. Met. Soc.*, *74*, 1335-1349, 1993.

Koster, R. and P. C. D. Milly, The interplay between transpiration and runoff formulations in land surface schemes used with atmospheric models, *J. Climate*, *10*, 1578-1591, 1997.

Koster, R.D., and M.J. Suarez, Modeling the land surface boundary in climate models as a composite of independent vegetation stands, *J. Geophys. Res.*, *97*, 2697-2715, 1992.

Koster, R. and M. Suarez, Energy and Water Balance Calculations in the Mosaic LSM, *NASA Tech. Memo.* 104606, Vol. 9, 1996.

Leung, L. R., and S. J. Ghan, A subgrid parameterization of orographic precipitation, *Theor. Appl. Climatol.*, *52*, 95-118, 1995.

Liang, X., D. P. Lettenmaier, E. F. Wood, and S. J. Burges, A simple hydrologically-based model of land surface water and energy fluxes for general circulation models, *J. Geophys. Res.*, *99*, 14415-14428, 1994.

Lynch-Stieglitz, M., The development and validation of a simple snow model for the GISS GCM, *J. Climate*, *7*, 1842-1855, 1994.

Manabe, S., Climate and the ocean circulation, I, The atmospheric circulation and the hydrology of the Earth's surface, *Mon. Weather Rev.*, *97*, 739-774, 1969.

Monteith, J.L., Evaporation and environment, *Symp. Soc. Exper. Biol.*, *19*, 205-234, 1965.

Pitman, A., A. Henderson-Sellers, and 38 others, Project for Intercomparison of Land-surface Parameterization Schemes, Results from offline control simulations (Phase 1a), *International GEWEX Project Office Publication Series No. 7*, GEWEX/WCRP, 47 pp., 1993.

Quinn, P., K. Beven, and A. Culf, The introduction of macroscale hydrological complexity into land surface-atmosphere transfer models and the effect on planetary boundary layer development, *J. Hydrol.*, *166*, 421-444, 1995a.

Quinn, P. K. Beven, and R. Lamb, The ln(a/tanβ) index, How to calculate it and how to use it within the TOPMODEL framework, *Hydrol. Process.*, *9*, 161-182, 1995b.

Robock, A., K. Y. Vinnikov, C. A. Schlosser, N. A. Speranskaya, and Y. K. Xue, Use of midlatitude soil moisture and meteorological observations to validate soil moisture simulations with biosphere and bucket models, *J. Climate*, *8*, 15-35, 1995.

Sellers, P. J., Y. Mintz, Y. C. Sud, and A. Dalcher, A simple biosphere model (SiB) for use within general circulation models, *J. Atmos. Sci.*, *43*, 505-531, 1986.

Sellers, P. J., D. A. Randall, G. J. Collatz, J. A. Berry, C. B. Field, D. A.

Dazlich, C. Zhang, G. D. Collelo, and L. Bounoua, A revised land surface parameterization (SiB2) for atmospheric GCMs, Part 1, Model formulation, *J. Climate*, *9*, 676-705, 1996.

Seth, A., F. Giorgi, and R. E. Dickinson, Simulating fluxes from heterogeneous land surfaces, Explicit subgrid method employing the biosphere-atmosphere transfer scheme (BATS), *J. Geophys. Res.*, *99*, 18651-18667, 1994.

Sivapalan, M., K. J. Beven, and E. F. Wood, On hydrologic similarity, 2, a scaled model of storm runoff production, *Water Resour. Res.*, *23(7)*, 1289-1299, 1987.

Stieglitz, M., D. Rind, J. Famiglietti, and C. Rosenzweig, An efficient approach to modeling the topographic control of surface hydrology for regional and global climate modeling, *J. Climate*, *10*, 118-137, 1997.

Wolock, D. M., and C. V. Price, Effects of digital elevation model map scale and data resolution on a topography-based watershed model, *Water Resour. Res.*, *30*, 3041-3052, 1994.

Verdin, K.L., and S. K. Jenson, Development of continental scale DEMs and extraction of hydrographic features, in *Proceedings: National Center for Geographic Information and Analysis (NCGIA) International Confer-*

ence/Workshop on Integrating GIS and Environmental Modeling, Santa Fe, New Mexico, January 21-25, 1996.

Verdin, K.L., and J.P. Verdin, A topological system for delineation and codification of the Earth's river basins, *J. Hydrol.*, *218*, 1-12, 1999..

Wolock, D. M., and G. J. McCabe, Comparison of single and multiple flow direction algorithms for computing topographic parameters in TOPMODEL, *Water Resour. Res.*, *31*, 1315-1324, 1995.

Wood, E.F., D. P. Lettenmaier, X. Liang, D. Lohmann, and 25 others, The project for the intercomparison of land-surface parameterization schemes (PILPS) phase 2(c) Red Arkansas river basin experiment, 1, Experiment description and summary intercomparisons, *J. Global and Planetary Change*, *19*, 115-135, 1998.

Zhang, W. and D. R. Montgomery, Digital elevation model grid size, the landscape representation, and hydrologic simulations, *Water Resour. Res.*, *30*, 1019-1028, 1994.

Figure Captions

Fig. 1 Illustration of catchment delineation in southwest North America. Overlain on the plot is a $4^\circ \times 5^\circ$ GCM grid.

Fig. 2 Illustration of the calculation of "catchment deficit", a bulk water variable used by the new LSM.

Fig. 3 Illustration of "root zone excess" at a point.

Fig. 4 Probability density functions (pdfs) of equilibrium root zone soil moisture at various catchment deficits in the catchment; see text for details.

Fig. 5 Thermal heat flux calculations in the catchment LSM. The same areal fraction of snowcover is assumed to lie over the saturated fraction (S), the transpiration fraction (T), and the wilting fraction (W). In each fraction, the ground surface exchanges heat with the snowcover and with the overlying atmosphere separately, and the snow surface itself exchanges heat with the atmophere. The three surface fractions exchange heat separately with an underlying ground layer, which in turn exchanges heat with lower ground layers.

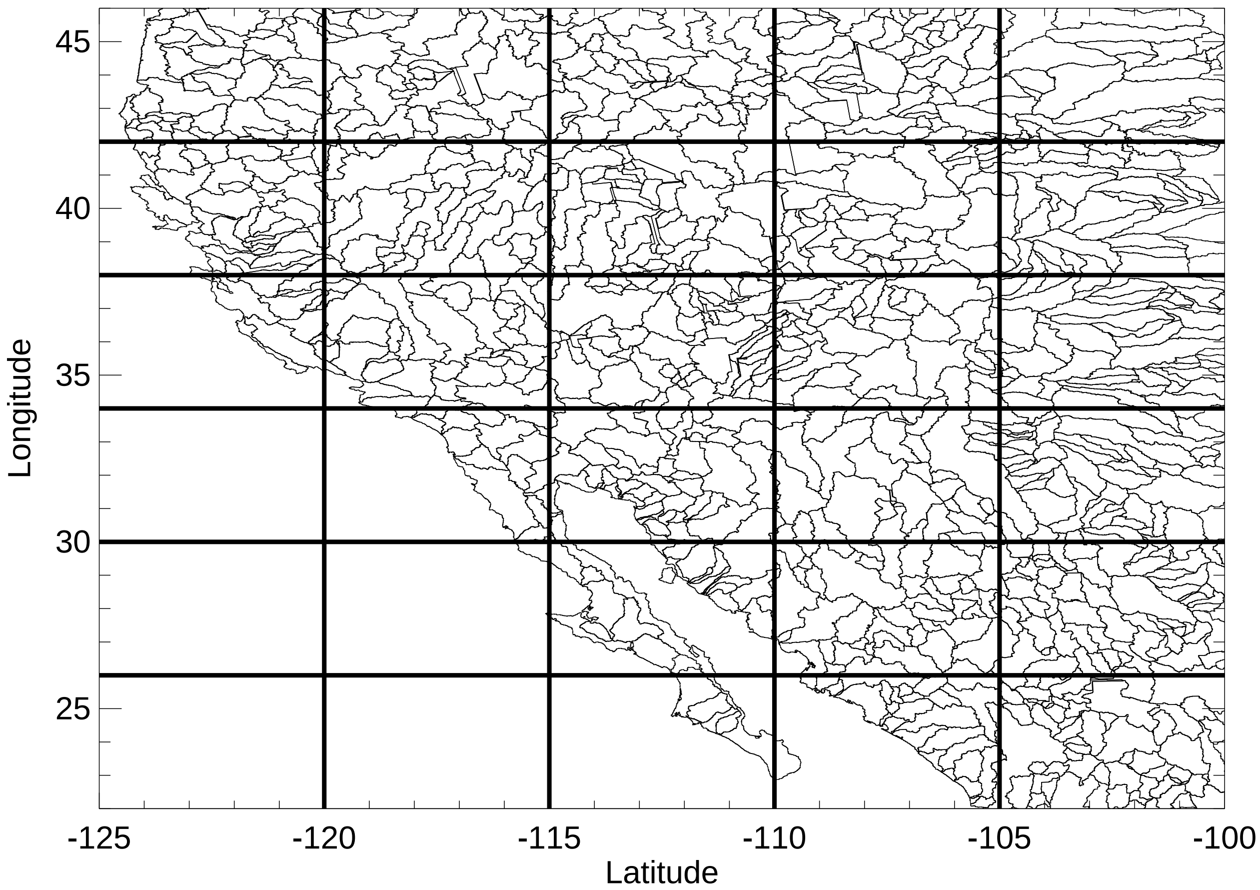

Figure 1: Illustration of catchment delineation in southwest North America. Overlain on the plot is a $4° \times 5°$ GCM grid.

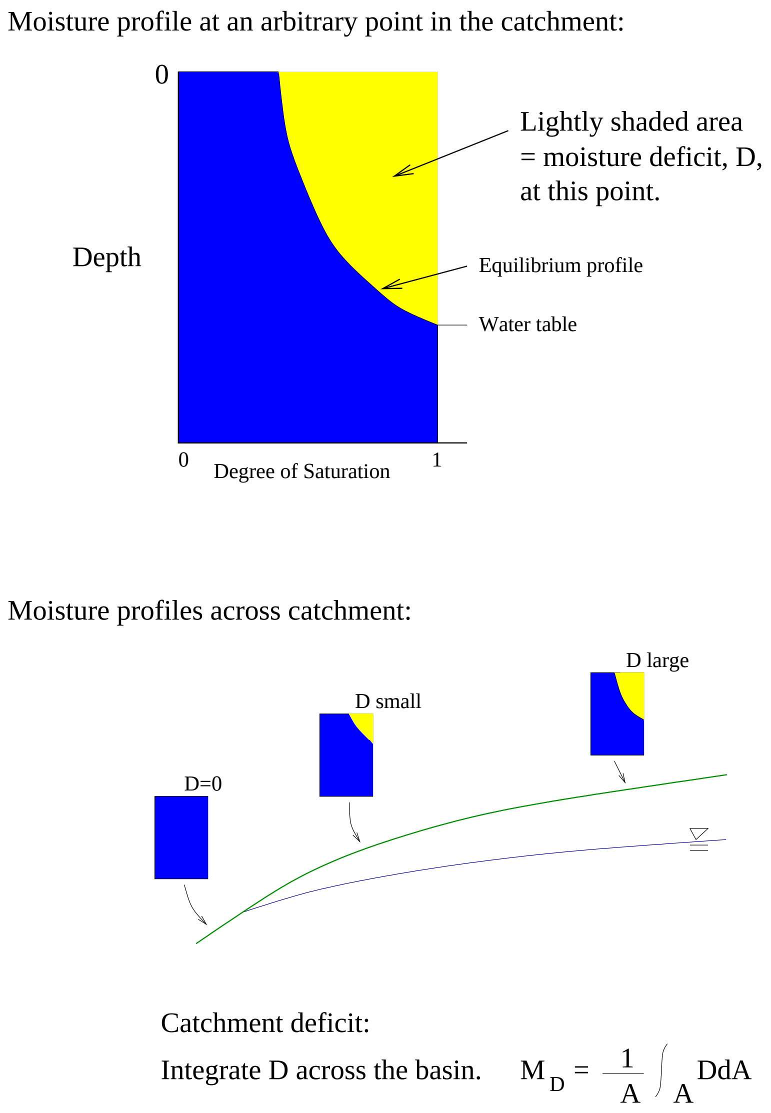

Figure 2: Illustration of the calculation of "catchment deficit", a bulk water variable used by the new LSM.

2ND SOIL MOISTURE PROGNOSTIC VARIABLE:
"ROOT ZONE EXCESS", M_{RZ}

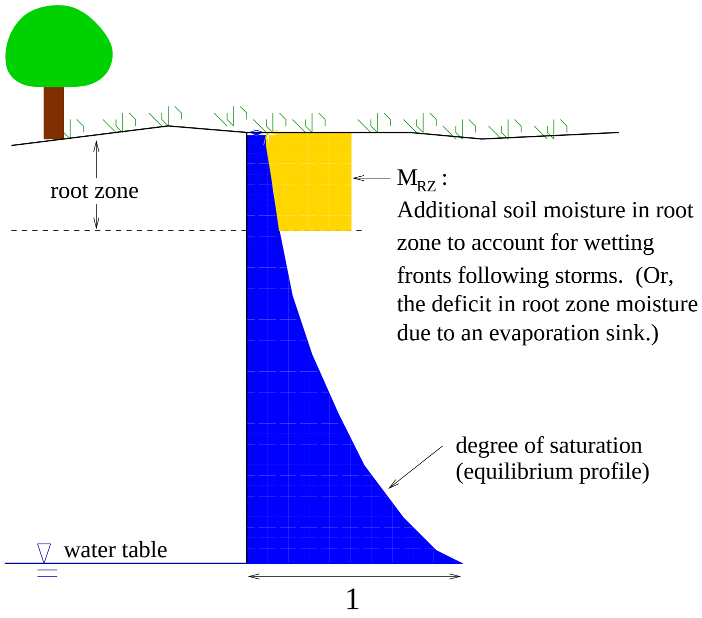

Figure 3: Illustration of "root zone excess" at a point.

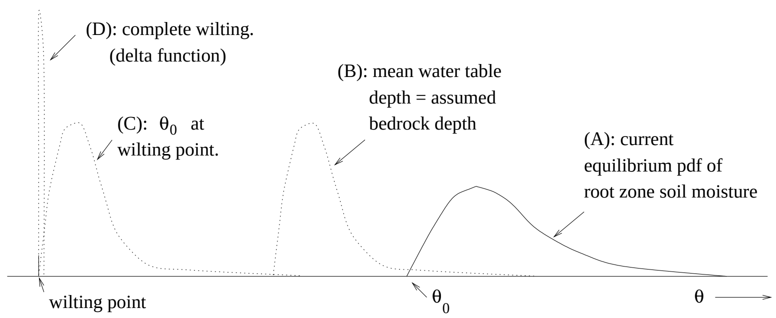

Figure 4: Probability density functions (pdfs) of equilibrium root zone soil moisture at various catchment deficits in the catchment; see text for details.

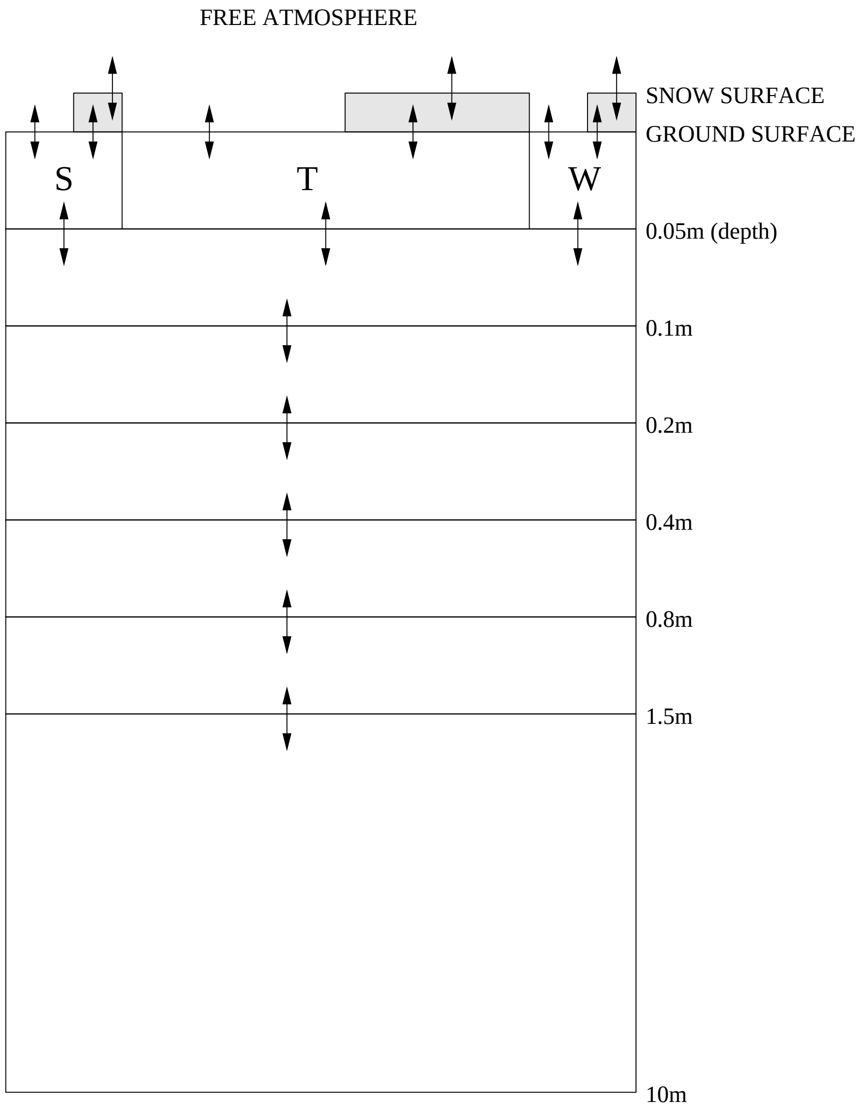

Figure 5: Thermal heat flux calculations in the catchment LSM. The same areal fraction of snowcover is assumed to lie over the saturated fraction (S), the transpiration fraction (T), and the wilting fraction (W). In each fraction, the ground surface exchanges heat with the snowcover and with the overlying atmosphere separately, and the snow surface itself exchanges heat with the atmophere. The three surface fractions exchange heat separately with an underlying ground layer, which in turn exchanges heat with lower ground layers.